

**$n = 5$  to  $n = 5$  soft-x-ray emission of uranium in a high-temperature low-density tokamak plasma**

Kevin B. Fournier, M. Finkenthal,\* S. Lippmann,† C. P. Holmes, and H. W. Moos  
*Department of Physics and Astronomy, The Johns Hopkins University, Baltimore, Maryland 21218*

W. H. Goldstein and A. L. Osterheld  
*L-Division, Lawrence Livermore National Laboratories, P.O. Box 808, Livermore, California 94550*  
 (Received 13 December 1993; revised manuscript received 8 August 1994)

The soft-x-ray uranium emission in the 60–200-Å range recorded from a high-temperature ( $\sim 1$  keV) low-density ( $\sim 10^{13}$  cm $^{-3}$ ) tokamak plasma has been analyzed by comparison with theoretical level structure and line-intensity calculations. In an extension of previous work [Finkenthal *et al.*, Phys. Rev. A **45**, 5846 (1992)], theoretical U XXV, U XXX, U XXXI, and U XXXII  $n = 5$  to  $n = 5$  spectra have been computed for the relevant plasma parameters. Fully relativistic parametric potential computer codes have been used for the *ab initio* atomic-structure calculations, and electron-impact excitation rates have been computed in the distorted-wave approximation.  $5s$ - $5p$  spectral lines and quasicontinua of U XXX, U XXXI, and U XXXII are identified in the 165–200-Å wavelength band. An unambiguous line identification is hampered by theoretical uncertainties and the blending of emission from adjacent charge states.

PACS number(s): 32.70.Fw, 31.20.Di

### INTRODUCTION

In a previous work, we presented the spectrum of uranium emitted from the high-temperature low-density TEXT tokamak (Center for Fusion Research, University of Texas at Austin) plasma in the 50–100 Å range [1]. The main emission features have been identified as due to  $n = 5$  to  $n = 5$  transitions within charge states having  $5p^6 5d^k$  ( $k = 1-10$ ) and  $5s^2 5p^n$  ( $n = 2-6$ ) ground configurations. The emission in that range was characterized by two relatively narrow groups of lines centered at approximately 70 and 88 Å. The identification of the arrays was based on *ab initio* relativistic level structure computations, and for the complex charge states, the unresolved-transition-array (UTA) model was used [2]. The present work extends the analysis of the uranium spectra by performing collisional-radiative model calculations for the U XXV (ground  $5s^2 5p^6$ ) to U XXXII ( $4f^{14} 5s$ ) ions emitting in the 60–200 Å range. Beyond the general spectroscopic interest in line identifications and comparison of the relativistic atomic-structure calculations with experiment, the charge states under discussion here are important because of their relevance to the study of a soft-x-ray laser scheme based on Nd I-like U XXXIII [3].

### EXPERIMENT

The experiments performed by Finkenthal (Ref. [1]) used the laser blow-off method [4] to introduce uranium atoms into hydrogen, deuterium, and helium tokamak

plasmas with central electron density and temperatures of  $2-4 \times 10^{13}$  cm $^{-3}$  and 1–1.5 keV, respectively. The spectra were recorded by a photometrically calibrated, time-resolving multispectral grazing incidence instrument [5], having a time resolution of 13.2 msec and a spectral resolution of 0.7 Å in the wavelength range from 50 to 200 Å. The uranium wavelengths have been established by poly-

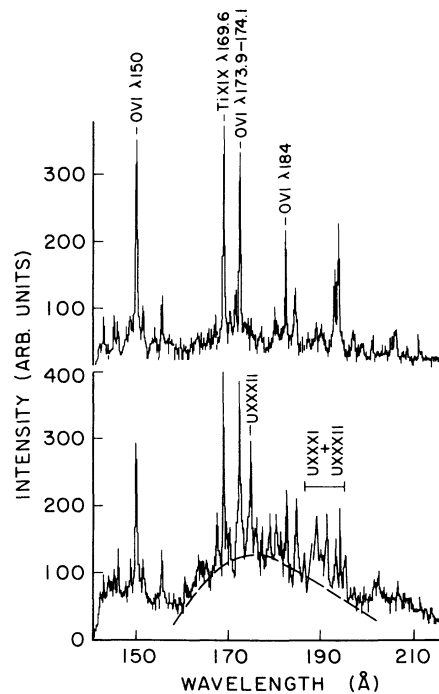


FIG. 1. The TEXT spectra recorded in the 150–200 Å range at uranium injection. Upper trace, intrinsic spectrum before injection. Lower trace, uranium and intrinsic spectra 40 msec after injection.

\*Permanent address: Racah Institute of Physics, The Hebrew University, Jerusalem, Israel.

†Permanent address: General Atomics, San Diego, CA 92186-9784.

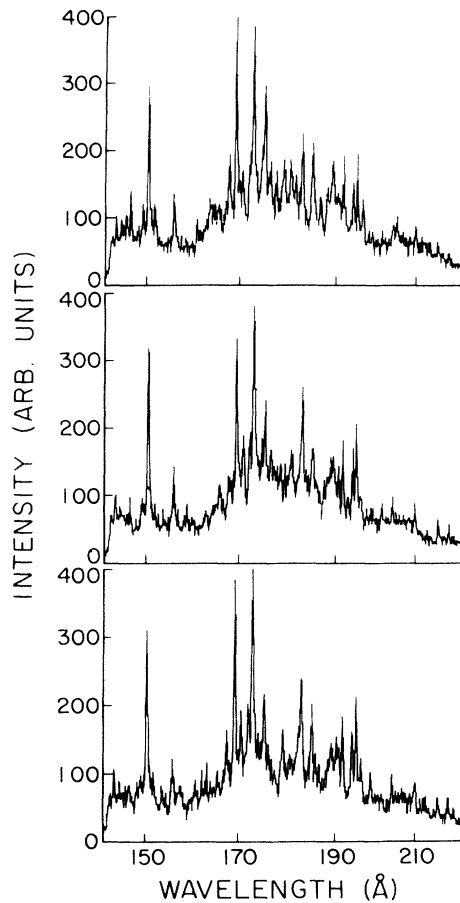


FIG. 2. Three uranium and intrinsic impurity spectra, each from a different discharge, at peak uranium emission in tokamak discharge with identical nominal parameters (plasma current, electron density, and temperature).

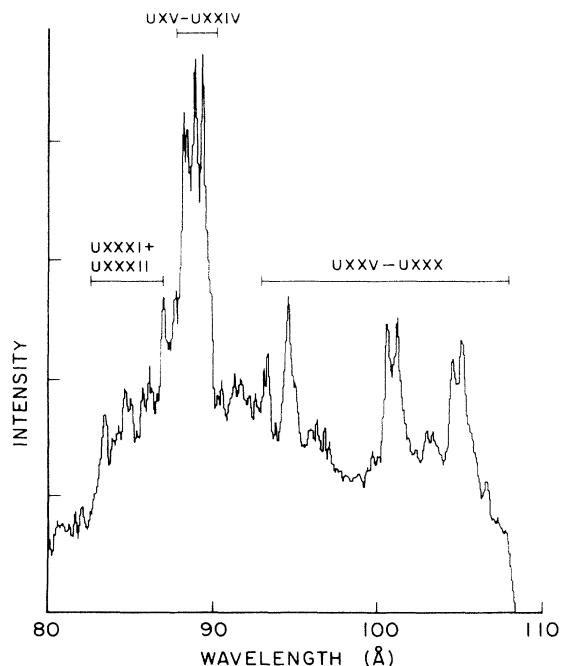


FIG. 3. Pure uranium spectrum in the 80–110 Å range, obtained by subtracting a preinjection frame from the frame of peak uranium emission at 88 Å.

nomial fits to the description equation using known intrinsic lines of oxygen and titanium; the estimated wavelength accuracy is 0.2 Å for unblended spectral features.

Figures 1 and 2 present experimental spectra recorded in the 150–200 Å range. The upper frame in Fig. 1 shows the intrinsic tokamak spectrum prior to the uranium injection, during the steady-state phase of the discharge. The lower figure shows the contribution of the uranium emission superimposed on the intrinsic spectrum. In Fig. 2, spectra recorded at the peak of uranium emission in three different discharges having nominally the same central electron density and temperature are shown to indicate the degree of reproducibility of the uranium emission. It is clear from these two figures that the strong line at 175.4 Å, several lines around 190 Å, and the overall background between 165 and 200 Å are due to uranium emission. In the actual analysis of the data we subtracted from the successive frames after uranium injection, and the frame before injection, and thus a pure uranium spectrum was obtained: Figures 3 and 4 present pure uranium spectra at the peak of the emission of highly ionized uranium in the 80–110 Å and 150–220 Å range, respectively.

#### CALCULATIONS

*Ab initio* level structure calculations have been performed for U XXV, XXX, XXXI, and XXXII (ions with relatively simple ground states,  $5p^65d$ ,  $5p^6$ ,  $5s^25p$ ,  $5s^2$ , and  $5s$ , respectively) using the parametric potential computer code RELAC [6]. For certain charge states, comparisons with level structure derived by Cowan's Hartree-Fock computer code with relativistic corrections have also been made [7]. Using the HULLAC package developed at Hebrew University and Lawrence Livermore Laboratory, a collisional-radiative model has been constructed for each of the four charge states mentioned above [8]. The package includes ANGLAR, which uses the graphical angular recoupling program NJGRAF to generate fine structure levels in a  $j-j$ -coupling scheme for a set of user-specified electron configurations [9]. ANGLAR then computes the angular part of the Hamiltonian for each ion and the tensor operators for radiative and collisional transitions. Next, RELAC generates wave functions and radiative transition probabilities. Finally, CROSS, a suite of three codes, is used to compute electron impact excitation cross sections and rate coefficients in the distorted-wave approximation [10]. Data from these codes then generates a collisional-radiative model which is solved in the steady state for level populations and line emissivities.

The HULLAC package has previously been used to generate collisional-radiative models for highly ionized heavy elements [11]. From the beginning, since this paper looks at very highly charged ions of heavy atoms, we have assumed that a fully relativistic approach to the calculations is better than a Hartree-Fock approach with relativistic corrections. For a comparison between relativistic and nonrelativistic methods with relativistic corrections, see Chap. 8 of Ref. [7]. Comparisons between RELAC and other fully relativistic codes have also been done [12]. There the authors concluded that there is no significant

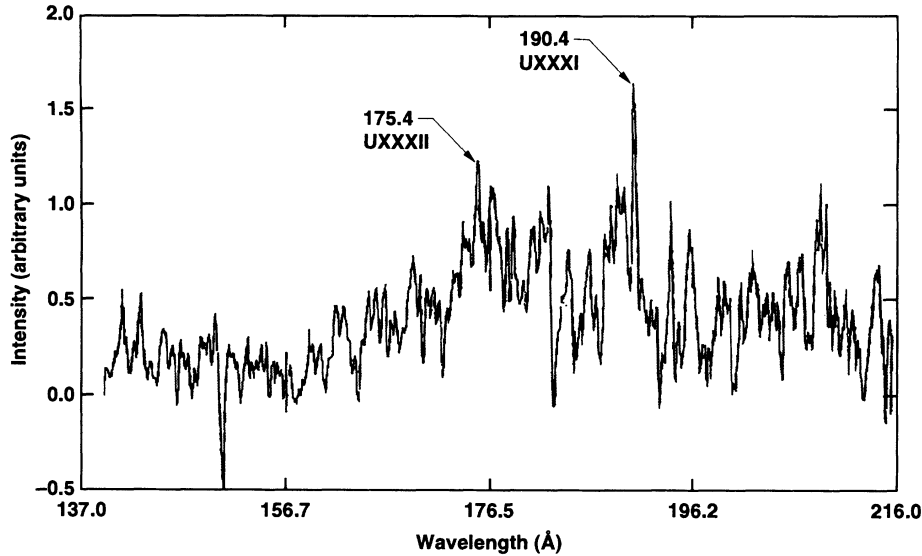


FIG. 4. Pure uranium spectrum in the 150–220 Å range, obtained by subtracting a preinjection frame from a frame 40 msec after the uranium injection.

difference between Grant's multiconfiguration Dirac-Fock (MCDF) code and the parametric potential method.

The output of the collisional-radiative model includes the level populations for each energy level in an ion relative to the ground-state population (marked  $n_i$  in Tables II–V below) and the relative intensity of radiative transitions from any given level to any other level (marked  $I$  in Tables II–V below). As can be seen in the tables, the lines with the highest transition probabilities are not necessarily the brightest in the spectrum. Also, since the computations are performed separately for each charge state, only the relative calculated intensities of the lines within a given charge state can be meaningfully com-

pared with the experiment. The fact that  $T_e$  was kept constant (at 1 keV) for lower charge states (such as U XXIV) should not affect the comparison because of the very slow decrease with temperature of the electron-impact excitation rates beyond their peak. The models contained 119, 140, 162, and 280 energy levels for U XXV, XXX, XXXI, and XXXII, respectively. More details on the computational procedure as well as on the results of the modeling are presented in Ref. [8].

## RESULTS

Table I lists experimental uranium lines and poses tentative identifications for some of those lines. Problems

TABLE I. Experimental wavelengths for  $n=5$  to  $n=5$  transitions in uranium ions and tentative identifications.

$\lambda(\text{\AA})$	Ion	Transition	Comments
70.0			
70.65			
71.7			
72.7		$5s^25p^k-5s5p^{k+1}$	
73.2			
73.8			
83.5	U XXV to U XXXII	and	See Ref. [1]
84.7			
86.2		$5s^k-5s^{k-1}5p$	
88.3		$5p^k-5p^{k-1}5d$	
89.0			
89.5			
94.6	U XXV	$5p^6-5p^55d$	blend with U XXIV
100.5	U XXV		See discussion in text
101.3	U XXV(?)		
104.6	U XXX	$5s^25p-5s^25d$	See discussion in text
105.2	U XXX(?)		
175.4	U XXXII	$5s-5p$	
188.5	U XXXII	$4f^{13}5s^2-4f^{13}5s5p$	See Ref. [8]
190.4	U XXXI	$5s^2-5s5p$	

TABLE II.  $5p$ - $5d$  and  $5d$ - $5f$  calculated transition wavelengths and collisional-radiative intensities in erbiumlike U XXV. The numbers in brackets denote multiplicative powers of ten.

Transition	$I = n_i^* A_{ij}$		Wavelength [Å]	
	[sec <sup>-1</sup> ]	[sec <sup>-1</sup> ] <sub>RELAC</sub>	RELAC	HF
$5s^2 5p^6 - 5s^2 5p^5 5d (J=1)$	3.1[05]	1.7[12]	67.48	71.98
$5s^2 5p^6 - 5s^2 5p^5 5d (J=1)$	4.1[05]	6.1[11]	93.73	100.99
$5s^2 5p^5 5d (J=3) - 5s^2 5p^5 5f (J=4)$	1.0[05]	6.3[11]	89.91	
$5s^2 5p^5 5d (J=4) - 5s^2 5p^5 5f (J=5)$	1.1[05]	7.2[11]	95.28	

with blends are indicated in the column labeled “Comments.” Issues unique to each charge state which affect the identification of special features are discussed below in the text.

The results of the computations show that for the U XXV ion, isoelectronic to erbium, with ground state  $5s^2 5p^6$ , the  $5p$ - $5d$  lines dominate the spectrum in the range of interest. Results are listed in Table II.

The collisional radiative model also yields two bright  $5d$ - $5f$  transitions whose wavelengths are well separated from the wavelength of the  $5p^6 - 5p^5_{3/2} 5d$  transition. For this ion, there is none of the configuration-interaction effect that blends and quenches the  $5p^6 5d^k - 5p^6 5d^{k-1} 5f$  and  $5p^6 5d^k - 5p^5_{3/2} 5d^{k+1}$  transitions of lower charge states as reported in Ref. [1], since the  $5p^5 5f$  and  $5p^5 5d$  configurations are of opposite parity and can not interact.

Wavelengths for the  $5p$ - $5d$  lines obtained in RELAC’s parametric potential model and from Hartree-Fock (HF) calculations differ significantly. The discrepancy has been traced to the interaction between the ground state and  $^1S_0$  components of the  $5p^5 6p$  configuration. Whereas RELAC calculates a mixing of about 4%, this interaction automatically vanishes in the Hartree-Fock treatment, since it involves configurations of the same symmetry differing in only one orbital. By dropping, *ad hoc*, the  $5p^6 - 5p^5 6p (^1S_0)$  interaction, RELAC predicts wavelengths of 71.48 and 101.86 Å for the  $5p$ - $5d$  transitions.

Without firm justification for neglecting the ground-state configuration interaction, we cannot resolve this discrepancy, and comparisons with measurements will be ambiguous at best. However, two possible sources can be identified for the overestimation in the parametric potential model. The first possibility is that the numerical accuracy of the present calculation is not sufficient in this case, where many integrals, representing interactions with each core orbital from  $1s$  through  $5s$ , are being added and subtracted to obtain what should presumably be a very small number. The second possibility is that the wavelength shift induced by the  $5p^5 6p$  interaction is canceled by interactions with all other  $^1S_0$  states, conceivably up to and including the continuum. Neither of these possibilities occur in the Hartree-Fock model, since the one-electron interaction is identically zero. Unfortunately, initial computational investigations do not support either possibility.

TABLE III.  $5p$ - $5d$  and  $5s$ - $5p$  calculated transition wavelengths and collisional-radiative intensities in europiumlike U XXX.

Transition	$I = n_i^* A_{ij}$		Wavelength [Å]	
	[sec <sup>-1</sup> ]	[sec <sup>-1</sup> ] <sub>RELAC</sub>	RELAC	HF
$5s^2 5p (J = \frac{1}{2}) - 5s^2 5d (J = \frac{3}{2})$	1.3[05]	1.2[12]	68.12	68.28
$5s^2 5p (J = \frac{3}{2}) - 5s^2 5d (J = \frac{5}{2})$	1.2[04]	1.8[11]	101.99	104.45
$5s^2 5p (J = \frac{1}{2}) - 5s 5p^2 (J = \frac{1}{2})$	9.3[04]	7.0[11]	85.37	84.69
$5s^2 5p (J = \frac{1}{2}) - 5s 5p^2 (J = \frac{3}{2})$	1.2[05]	3.8[11]	86.38	85.26
$5s^2 5p (J = \frac{1}{2}) - 5s 5p^2 (J = \frac{5}{2})$	5.6[04]	2.8[10]	182.45	
$5s^2 5p (J = \frac{3}{2}) - 5s 5p^2 (J = \frac{3}{2})$	1.4[04]	1.4[10]	192.22	

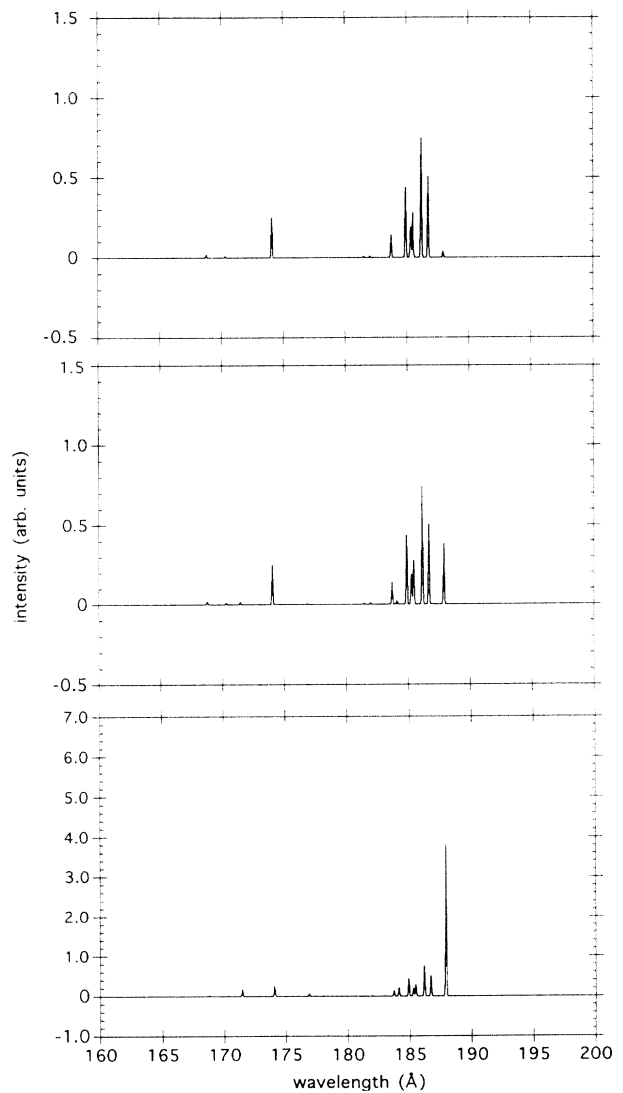


FIG. 5. Synthetic U XXXI–U XXXII spectra in the long-wavelength range showing the effect of various fractional abundances of the two charge states (U XXXI to U XXXII, respectively) on the relative intensities of the lines in Tables IV and V: top frame: 1:10; middle frame: 1:1; bottom frame: 10:1.

TABLE IV.  $5s$ - $5p$  calculated transition wavelengths and collisional-radiative intensities in samariumlike U XXXI.

Transition	$I=n_i^* A_{ij}$	$A_{ij}$	Wavelength	
	[ $\text{sec}^{-1}$ ]	[ $\text{sec}^{-1}$ ]	RELAC	HF
$5s^2$ - $5s5p$ ( $J=1$ )	2.5[05]	6.0[11]	85.99	85.16
$5s^2$ - $5s5p$ ( $J=1$ )	1.4[05]	1.7[10]	187.93	193.48

The experimental spectra show two strong features at 100.5 and 101.3 Å (see Fig. 3); they appear together in time with the 70 and 88 Å structures, indicating that they are from charge states nearby to those causing the bands. Because of the uncertainty in the wavelengths of our calculations, and because both features seem equally bright, thus not helping us decide which line is from a strong resonance transition, a firm statement as to which feature corresponds to the  $5p^6$ - $5p_{3/2}^5 5d$  transition is impossible.

TABLE V.  $5s$ - $5p$  and  $5s^2$ - $5s5p$  calculated transition wavelengths and collisional-radiative intensities in promethiumlike U XXXII

Transition	$I=n_i^* A_{ij}$	$A_{ij}$	Wavelength	
	[ $\text{sec}^{-1}$ ]	[ $\text{sec}^{-1}$ ]	RELAC	HF
$4f^{14}5s$ ( $J=\frac{1}{2}$ )- $4f^{14}5p$ ( $J=\frac{3}{2}$ )	1.2[05]	4.0[11]	86.06	
$4f^{14}5s$ ( $J=\frac{1}{2}$ )- $4f^{14}5p$ ( $J=\frac{1}{2}$ )	9.5[04]	4.9[10]	174.11	
$4f^{13}5s^2$ ( $J=\frac{7}{2}$ )- $4f^{13}5s5p$ ( $J=\frac{7}{2}$ )	4.1[05]	6.3[11]	82.75	
$4f^{13}5s^2$ ( $J=\frac{7}{2}$ )- $4f^{13}5s5p$ ( $J=\frac{5}{2}$ )	5.5[04]	1.0[11]	83.39	
$4f^{13}5s^2$ ( $J=\frac{7}{2}$ )- $4f^{13}5s5p$ ( $J=\frac{9}{2}$ )	3.1[05]	3.6[11]	83.72	
$4f^{13}5s^2$ ( $J=\frac{5}{2}$ )- $4f^{13}5s5p$ ( $J=\frac{7}{2}$ )	2.0[05]	6.1[11]	83.89	
$4f^{13}5s^2$ ( $J=\frac{7}{2}$ )- $4f^{14}5s5p$ ( $J=\frac{5}{2}$ )	2.6[05]	5.0[11]	84.21	
$4f^{13}5s^2$ ( $J=\frac{7}{2}$ )- $4f^{13}5s5p$ ( $J=\frac{9}{2}$ )	2.4[05]	2.6[11]	84.45	
$4f^{13}5s^2$ ( $J=\frac{7}{2}$ )- $4f^{13}5s5p$ ( $J=\frac{5}{2}$ )	1.6[05]	1.8[10]	184.91	
$4f^{13}5s^2$ ( $J=\frac{7}{2}$ )- $4f^{13}5s5p$ ( $J=\frac{9}{2}$ )	2.7[05]	1.7[10]	186.18	
$4f^{13}5s^2$ ( $J=\frac{7}{2}$ )- $4f^{13}5s5p$ ( $J=\frac{7}{2}$ )	1.8[05]	1.5[10]	186.72	

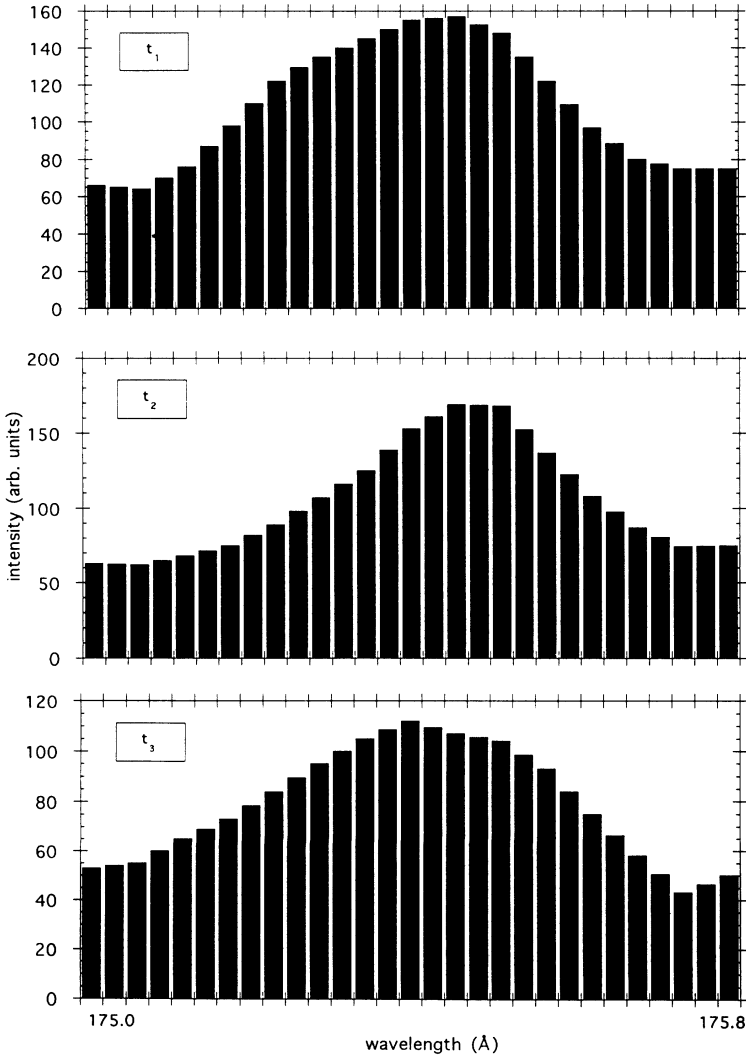


FIG. 6. The spectral profile of the UXXXII line at 175.4 Å: the top trace ( $t_1$ ) is at the peak of uranium emission, and the following two frames ( $t_2$  and  $t_3$ ) are at successive intervals (13.2 msec apart).

Also, the experimental spectra show a strong feature at 94.6 Å (Fig. 3); it, too, appears together with the 70 and 88 Å structures; the width of the line is larger than that of an individual line, and probably indicates a blend of the predicted 95.28 Å feature (predicted wavelength without the ground-state configuration interaction) with lines from lower charge states.

In the case of U XXX, isoelectronic to europium, with ground-state  $5s^25p$ ,  $5p-5d$ , and  $5s-5p$  transitions, will appear as strong lines in the spectral range under consideration (Table III). The  $5p-5d$  line predicted at 68.12 Å is in the 70 Å array; the  $5s-5p$  lines at 85 and 86 Å are subsumed in the array at 88 Å. The two somewhat weaker  $5s-5p$  lines at longer wavelengths are part of the forest of weaker lines which constitute the background between 170 and 190 Å (see Fig. 1 and the discussion in connection with U XXXI and U XXXII emission). The discrepancy between the RELAC and HF wavelengths is less here for the longer wavelength  $5p-5d$  transition than in the case of U XXV, but still significant in magnitude. Since we measure in the spectra two lines at 101.3 and 104.6 Å (Fig. 3) it is difficult to decide which of the two belongs to U XXX.

The ground state of the ion U XXXI, isoelectronic to samarium, is  $4f^{14}5s^2$ . The strongest lines are expected to be those from the  $5s^2^1S_0-5s5p^1P_1, ^3P_1$  transitions. These are shown in Table IV. The resonance  $^1S_0-^1P_1$  line is predicted by RELAC at 85.99 Å and by the HF calculations at 85.16 Å. As one can see in Fig. 3, the line at 85 Å is blended with the transitions emitted by the lower charge states discussed in Ref. [1] and some U XXXII lines discussed below. The intercombination line, predicted at 188 (RELAC) and 193 Å (HF), would be one of the lines in the group around 190 Å; we tend to identify it as the 190.4 Å line (Fig. 4), because of its reproducibility in all uranium spectra and its rather high intensity. (Although the spectral feature at 190.4 Å is present in all uranium injections, its shape and intensity varies slightly between discharges, as seen in Fig. 2).

The next charge state U XXXII, isoelectronic to promethium, also has a simple ground-state

configuration,  $4f^{14}5s$ . However, just about 150 eV above the ground one finds the metastable  $4f^{13}5s^2$  state. This can be populated either by electron excitation from the ground, or by inner-shell ionization (of a  $4f$  electron) from the ground state of the U XXXI ion. Since there is no radiative decay from these levels to the ground state or the excited  $4f^{14}5p$  state, an entire array of  $4f^{13}5s^2-4f^{13}5s5p$  transitions will be emitted as satellites of the resonance  $5s-5p$  transition. Table V summarizes the results of the predictions of the collisional radiative calculations for this charge state. The surprising result of these calculations is that some of the transitions to the metastable levels are predicted to be brighter than the resonance  $5s-5p$  transitions. The same result is presented graphically in the 160–200 Å range in Fig. 5, where the collisional radiative model calculations are plotted at  $n_e = 10^{13} \text{ cm}^{-3}$  and  $T_e = 1 \text{ keV}$  for U XXXI and U XXXII for different relative abundances. Once again, we cannot distinguish between the individual transitions around 88 Å; at longer wavelengths, in contrast, we identify the line at 175.4 Å (Fig. 4) as originating from the  $5s^2S_{1/2}-5p^2P_{1/2}$  transition. As seen from Figs. 1 and 2 this line is clearly a uranium line. Moreover, Fig. 6 shows the position of the peak and width of the line in three consecutive frames; as one can see, the variation in the peak position is smaller than the 0.2 Å resolution limit of the experiment. The width of the line seems to broaden at later times, but this is due to the poor signal-to-noise ratio in this later frame. Figure 7 shows the time history of the 175.4 Å line: as expected for a high charge state, the signal rises over several tens of milliseconds and decays on a similar time scale.

There are many weaker lines around 185–190 Å. Since it is difficult to classify specific lines by our collisional-radiative models, we will only state here that from comparison with theoretical spectra and the actual time history of the lines, we conclude that they belong to the U XXX–U XXXII ions. The uranium emission hump between 170 and 190 Å is due to the transitions shown in Tables III–V and, to a much lesser extent, to the second-order emission of the structure at 88 Å.

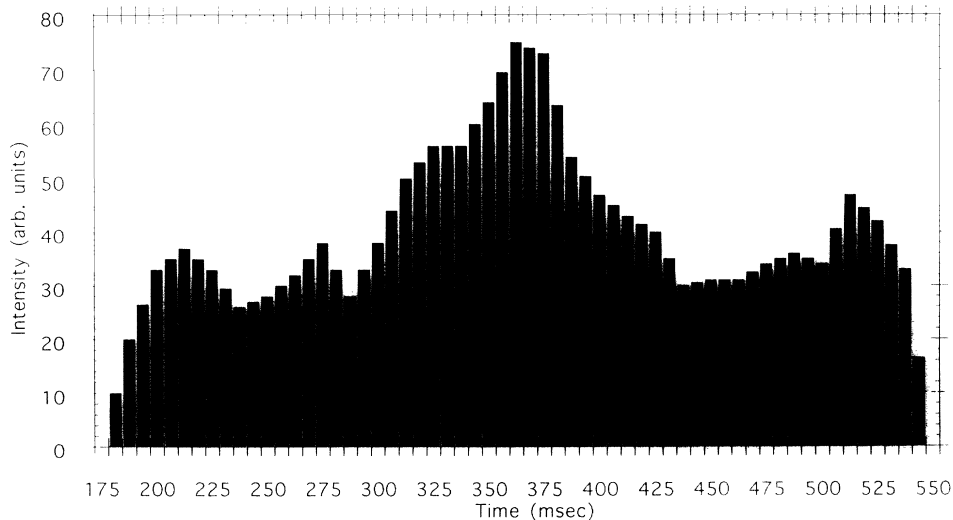


FIG. 7. Time history of the 175.4 Å line over a 350-msec period.

## CONCLUSION

We have measured several uranium emission lines in a low-density tokamak plasma, and have tentatively identified some of the strongest U XXV–U XXXII transitions in the 80–190 Å range, connecting the low-lying excited states to the ground states. The lack of isoelectronic data and the relatively low spectral resolution of the present experiment do not enable a rigorous classification of the individual transitions; however, the good agreement between the *ab initio* energy-level calculations, the collisional-radiative line intensity predictions, and the experiment over this large range of charge states support the present analysis. The low-density tokamak plasma emits a much more structured spectrum of the highly ionized heavy atoms than the laser-produced plasma due to the fact that only levels close to the ground state are significantly populated and radiation trapping is absent. This enables the straightforward comparison between the experiment and the described theoretical computations. The time-resolved nature of our data lets us identify which charge states are making up the quasicontinua in the 165–200 Å range. Further, the collisional-radiative models let us identify the strong  $5s-5p$  transitions in this

region for U XXX, XXXI, and XXXII. At shorter wavelengths, definitive statements about the identity of spectral features are hard to make, because of the crowded spectral region around 88 Å and the fact that we have to rely on an *ad hoc* modification to our calculations to obtain good agreement with other calculation methods. Overall, at longer wavelengths, the good agreement between the data and calculations gives confidence in the calculations' use in the modeling of the much more complex, high-density, laser and/or pulsed power produced plasmas.

## ACKNOWLEDGMENTS

We would like to acknowledge Dr. A. Zwicker and Dr. L. K. Huang and the TEXT group for their help in the described experiments, and Dr. V. Kaufman for providing the HF calculations. The present work was performed under the auspices of the U.S. Department of Energy by contract between the Plasma Spectroscopy Group at Johns Hopkins University and the Lawrence Livermore National Laboratories under Contract No. W-7405-ENG-48.

- 
- [1] M. Finkenthal, S. Lippmann, H. W. Moos, P. Mandelbaum, and the TEXT Group, *Phys. Rev. A* **39**, 3717 (1989).
- [2] J. Bauche, C. Bauche-Arnoult, M. Klapisch, P. Mandelbaum, and J. L. Schwob, *J. Phys. B* **20**, 1443 (1987).
- [3] P. L. Hagelstein and S. Dalhed, *Phys. Rev. A* **37**, 1357 (1988).
- [4] E. Marmor, J. Cecchi, and S. Cohen, *Rev. Sci. Instrum.* **46**, 1149 (1975).
- [5] W. L. Hodge, B. C. Stratton, and H. W. Moos, *Rev. Sci. Instrum.* **55**, 6 (1984).
- [6] M. Klapisch, *Comput. Phys. Commun.* **2**, 269 (1971); M. Klapisch, J. L. Schwob, B. S. Fraenkel, and J. Oreg, *J. Opt. Soc. Am.* **67**, 148 (1977).
- [7] V. Kaufman (private communication). For details about the Hartree-Fock method and codes, see also R. Cowan, *The Theory of Atomic Structure and Spectra* (University of California Press, Berkeley, 1981).
- [8] K. Fournier, W. H. Goldstein, A. L. Osterheld, M. Finkenthal, C. Holmes, and H. W. Moos, UCRL Report No. 115497, 1993 (unpublished).
- [9] A. Bar-Shalom and M. Klapisch, *Comput. Phys. Commun.* **50**, 375 (1988).
- [10] A. Bar-Shalom, M. Klapisch, and J. Oreg, *Phys. Rev. A* **38**, 1773 (1988).
- [11] M. Finkenthal, S. Lippman, L. K. Huang, A. Zwicker, H. W. Moos, W. H. Goldstein, and A. L. Osterheld, *Phys. Rev. A* **45**, 5846 (1992).
- [12] P. Quinet and E. Biemont, *Phys. Scr.* **43**, 150 (1991).

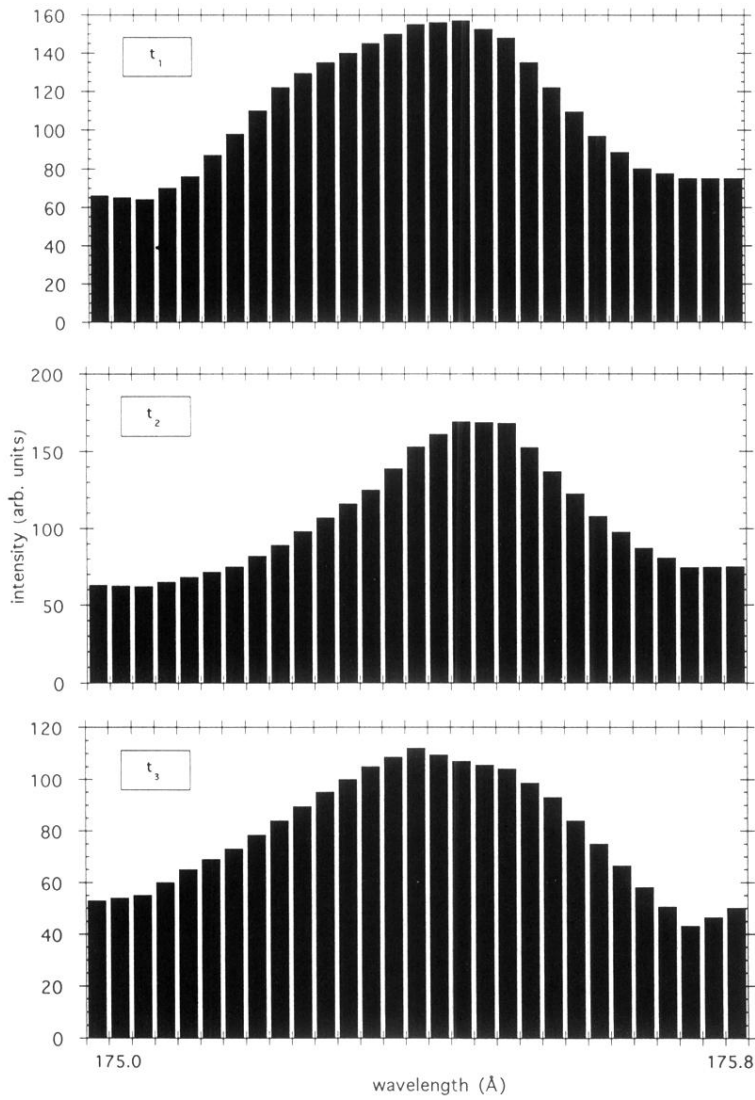


FIG. 6. The spectral profile of the UXXXII line at 175.4 Å: the top trace ( $t_1$ ) is at the peak of uranium emission, and the following two frames ( $t_2$  and  $t_3$ ) are at successive intervals (13.2 msec apart).



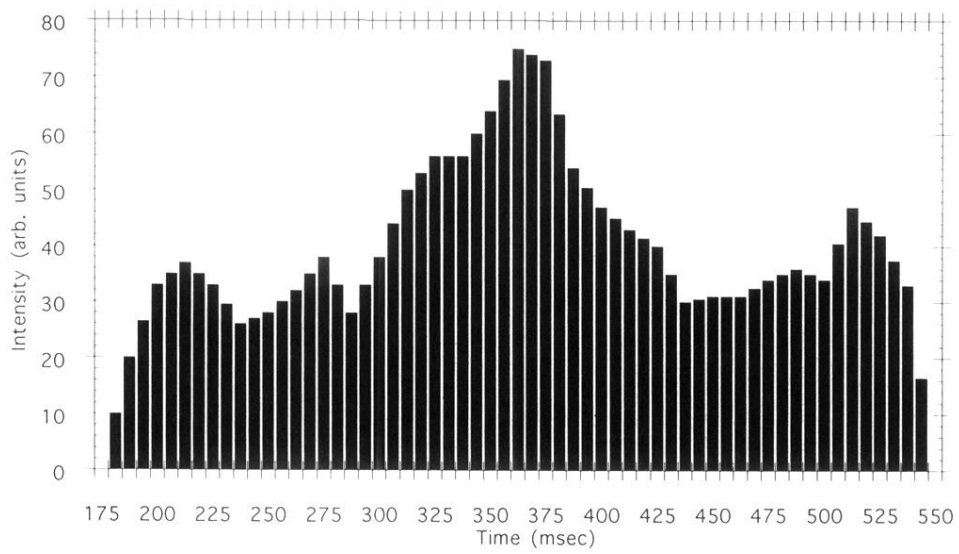


FIG. 7. Time history of the 175.4 Å line over a 350-msec period.